Author Manuscript

Author Manuscript

Author Manuscript

Author Manuscript

HHS Public Access

Author manuscript

Circulation. Author manuscript; available in PMC 2023 September 27.

Published in final edited form as:

Circulation. 2022 September 27; 146(13): 1028–1031. doi:10.1161/CIRCULATIONAHA.122.059594.

Mitochondrial stress induces an HRI-eIF2α pathway protective for cardiomyopathy

Siting Zhu, BS[1,2,¶], **Anh Nguyen, BS**[1,¶], **Jing Pang, BS**[1,¶], **Jun Zhao, PhD**[3], **Ze'e Chen, PhD**[1,2], **Zhengyu Liang, PhD**[1], **Yusu Gu, MS**[1], **Helen Huynh, BS**[1], **Yutong Bao, BS**[1], **Sharon Lee, BS**[1], **Yuval Kluger, PhD**[3], **Kunfu Ouyang, PhD**[2], **Sylvia M Evans, PhD**[1,4,5], **Xi Fang, PhD**[1,*]

[1]Department of Medicine, University of California San Diego, La Jolla, California, USA

[2]Department of Cardiovascular Surgery, Peking University Shenzhen Hospital, School of Chemical Biology and Biotechnology, State Key Laboratory of Chemical Oncogenomics, Peking University Shenzhen Graduate School, Shenzhen, China.

[3]Department of Pathology, Yale School of Medicine, New Haven, CT, USA

[4]Department of Pharmacology, University of California San Diego, La Jolla, California, USA

[5]Skaggs School of Pharmacy and Pharmaceutical Sciences, University of California San Diego, La Jolla, California, USA

Mitochondrial dysfunction elicits a mitochondrial stress response (MSR) through mitochondrial-nuclear communication and activates ATF4, a master transcriptional regulator of the cellular stress response[1]. Knowledge of consequences of MSR-triggered ATF4 activation in mitochondrial cardiomyopathy is limited, yet critical for therapeutic approaches.

Mitochondrial phosphatase *Ptpmt1* cKO mice (PKO)[2] provide a model to investigate *in vivo* mechanisms of MSR in cardiomyocytes, displaying key features of fetal mitochondrial cardiomyopathy, while evidencing lethality between E16.5–18.5[2]. All mouse protocols were approved by the Institutional Animal Care and Use Committee. Molecular analyses confirmed that loss of PTPMT1 in cardiomyocytes resulted in upregulation of ATF4 and its target genes at E11.5 (Figure A–D), similar to other MSR models. The most well recognized upstream regulator of ATF4 is eIF2α phosphorylation, which increases ATF4 translation. *Atf4* is also a direct target of transcriptional repression by HIF1α in cardiomyocytes. *Hif1*α cKO hearts display increased *Atf4* mRNA and protein. mTOR is another upstream regulator of ATF4. We examined these upstream regulators of ATF4 in PKO hearts, and found that phosphorylation of eIF2α was significantly increased in PKO versus control hearts at E11.5,

*Correspondence to Xi Fang, PhD, Department of Medicine, University of California San Diego, 9500 Gilman Dr., Mail Code 0613-C, La Jolla, CA 92093. xifang@ucsd.edu. Phone: 858-822-4276.

¶The first three authors contributed equally to the study.

Disclosures

Jun Zhao is currently employed by Guardant Health, US. This work is not related to her employment at Guardant Health.

Author Manuscript Author Manuscript Author Manuscript Author Manuscript

while HIF1α and mTOR phosphorylation were not altered (Figure E), suggesting that eIF2α phosphorylation induced expression of ATF4.

Phosphorylation of eIF2α at serine 51 integrates signals from diverse cellular stress responses (Figure F)[1]. We generated a "phosphorylation-resistant" eIF2α mutant allele[1], in which the serine 51 phosphorylation site was mutated to alanine (eIF2α^{S51A}), and crossed this allele into PKO mice to generate PKO/eIF2α^{S51A} double mutant mice (dMut). Absence of eIF2α phosphorylation in eIF2α^{S51A} and dMut hearts was validated (Figure G). ATF4 protein and downstream targets were significantly decreased to baseline levels in dMut hearts (Figure G–I), confirming that eIF2α phosphorylation was essential for MSR-triggered ATF4 activation in PKO hearts.

Four eIF2α kinases are activated by distinct forms of stress (Figure F)[1]. RNA-seq analysis from PKOs indicated increased expression of ATF4 targets, but no increase in XBP1- or ATF6 (Figure J), the latter negating the likelihood that a PERK-mediated stress response was involved[1]. Next, we generated null alleles for GCN2 or HRI, and generated PKO/GCN2 and PKO/HRI double knockout mice (dKO). Loss of HRI abolished activation of eIF2α-ATF4 signaling in PKOs, while eIF2α-ATF4 remained activated in PKO/GCN2 dKO hearts (Figure K–O). Thus, MSR induced eIF2α-ATF4 signaling was dependent on HRI, while other eIF2α kinases were not involved. Our results are consistent with recent *in vitro* findings in HeLa cells[3,4], providing the first demonstration of the *in vivo* relevance of this pathway in mitochondrial cardiomyopathy. It is not clear whether activation of HRI depends on the amount of heme in cardiomyocytes.

Whether the eIF2α pathway was adaptive or maladaptive remained to be addressed. Although global suppression of protein synthesis by eIF2α phosphorylation conserves energy, and increasing ATF4 translation allows cells to survive periods of stress, persistent ATF4 and suppression of protein synthesis may also be detrimental. Homozygous eIF2α^{S51A} mutants die within 18 hours after birth[1]. However, constitutive activation of eIF2α by deleting both eIF2α phosphatases *Ppp1r15a* and *Ppp1r15b* results in embryonic lethality[1]. Thus far, *in vivo* physiological consequences of eIF2α phosphorylation in response to stress have not been addressed. We analyzed morphology and survival of PKO/eIF2α^{S51A} dMut mice. PKO/eIF2α^{S51A} dMut mice died at E13.5, while PKO mice survived at this stage with abnormal heart morphology, demonstrating that blocking eIF2α phosphorylation negatively impacted survival (Figure P).

Although HRI null mice were viable[1] and displayed normal cardiac development and function at baseline, the role of HRI activation in mitochondrial cardiomyopathy remained to be addressed. We found that PKO/HRI dKOs died between E14.5-E16.5, while PKO littermates survived with abnormal cardiac morphology (Figure Q). Thus, although milder than effects of the eIF2α S51A mutant, deletion of HRI was also detrimental to survival. Thus HRI-eIF2α activation was protective for fetal mitochondrial cardiomyopathy

To determine the role of HRI in adult mitochondrial cardiomyopathy, we crossed HRI knockout mice with *Tafazzin* cKO (TKO) mice. TKO mice display mitochondrial dysfunction at 2 months and dilated cardiomyopathy at 4 months, but survive more than

Author Manuscript Author Manuscript Author Manuscript Author Manuscript

one year with impaired cardiac function[5]. Western blot and qPCR analysis confirmed that eIF2α-ATF4 signaling was activated in TKO hearts but abolished in TKO/HRI dKO hearts (Figure R–S). TKO/HRI dKO mice died between postnatal day (P) 7–10 with enlarged hearts, compared to TKO mice that survived more than one year[5]. We also observed increased ventricular weight to body weight ratios in dKOs (Figure T–U). Echocardiographic analysis revealed severe cardiac dysfunction in dKOs (Figure V). Thus, MSR triggered HRI-eIF2α was also protective for adult mitochondrial cardiomyopathy.

Overall we demonstrated that an HRI-eIF2α pathway mediated mitochondrial-nuclear communication and MSR-triggered ATF4 activation in both embryonic and adult heart. Our results uncovered a protective role for MSR triggered HRI-eIF2α-ATF4 signaling in both fetal and adult mitochondrial cardiomyopathy. Therefore, intention to inhibit the HRI-eIF2α-ATF4 pathway in mitochondrial cardiomyopathy could be detrimental, rather than beneficial, for cardiac dysfunction.

The data, analytical methods, and study materials that support the findings of this study will be available to other researchers from the corresponding authors on reasonable request. RNAseq data was deposited to the GEO database (Accession number: GSE201042).

Sources of Funding

XF is supported by NIH grants. SME is supported by NIH grants and the Foundation Leducq (16 CVD 03).

Reference:

1. Costa-Mattioli M and Walter P. The integrated stress response: From mechanism to disease. Science. 2020 Apr 24;368(6489):eaat5314. [PubMed: 32327570]
2. Chen Z, Zhu S, Wang H, Wang L, Zhang J, Gu Y, Tan C, Dhanani M, Wever E, Wang X, Xie B, Wang S, Huang L, van Kampen AHC, Liu J, Han Z, Patel HH, Vaz FM, Fang X, Chen J and Ouyang K. PTPMT1 Is Required for Embryonic Cardiac Cardiolipin Biosynthesis to Regulate Mitochondrial Morphogenesis and Heart Development. Circulation. 2021;144:403–406. [PubMed: 34339306]
3. Fessler E, Eckl EM, Schmitt S, Mancilla IA, Meyer-Bender MF, Hanf M, Philippou-Massier J, Krebs S, Zischka H and Jae LT. A pathway coordinated by DELE1 relays mitochondrial stress to the cytosol. Nature. 2020;579:433–437. [PubMed: 32132706]
4. Guo X, Aviles G, Liu Y, Tian R, Unger BA, Lin YT, Wiita AP, Xu K, Correia MA and Kampmann M. Mitochondrial stress is relayed to the cytosol by an OMA1-DELE1-HRI pathway. Nature. 2020;579:427–432. [PubMed: 32132707]
5. Zhu S, Chen Z, Zhu M, Shen Y, Leon LJ, Chi L, Spinozzi S, Tan C, Gu Y, Nguyen A, Zhou Y, Feng W, Vaz FM, Wang X, Gustafsson AB, Evans SM, Kunfu O and Fang X. Cardiolipin Remodeling Defects Impair Mitochondrial Architecture and Function in a Murine Model of Barth Syndrome Cardiomyopathy. Circ Heart Fail. 2021;14:e008289. [PubMed: 34129362]

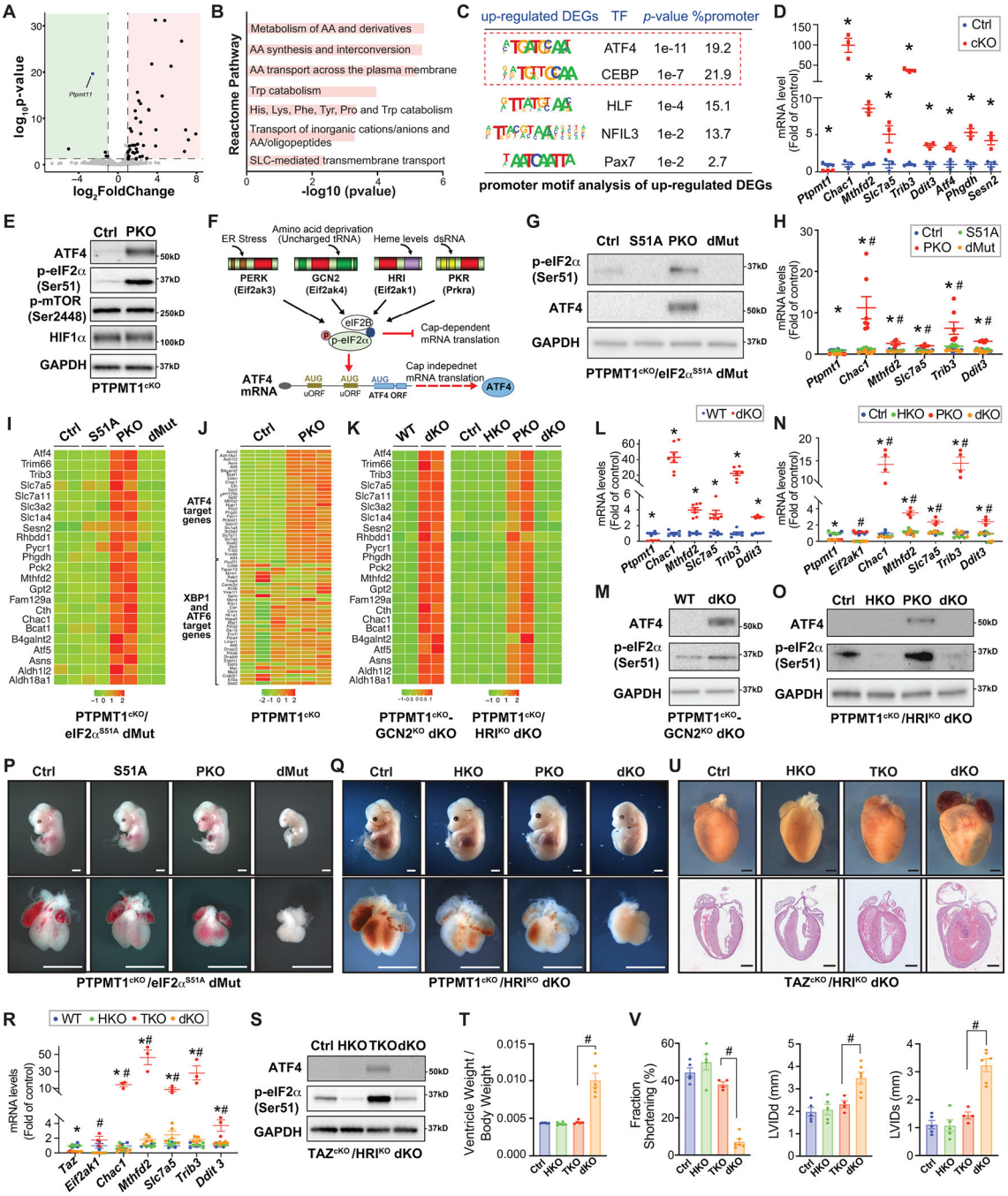

Figure.

A. Volcano plot obtained from DESeq2 analysis of gene expression in *Ptpmt1* cardiomyocyte-specific knockout (*Ptpmt1*$^{f/f}$; *Xml*-Cre^{+}; PKO) versus Cre negative control hearts at E11.5. Genes with adjusted P<0.05 and log2 (fold change) >1 are considered significantly upregulated or downregulated genes in PKO hearts. Green indicates downregulated genes; red indicates upregulated genes. n=3 per group. RNAseq data was deposited to the GEO database (Accession number: GSE201042). **B.** Functional clustering analysis utilizing the Reactome database revealed that deletion of PTPMT1 in

Author Manuscript Author Manuscript Author Manuscript Author Manuscript

Author Manuscript Author Manuscript Author Manuscript Author Manuscript

cardiomyocytes significantly upregulates pathways involved in amino acid metabolism, which is classically found to be regulated by ATF4. AA: amino acid; Trp: tryptophan; His: histidine; Lys: lysine; Phe: phenylalanine; SLC: solute carrier superfamily. **C.** Motif enrichment analysis at promoter regions (±2 kb from transcription start sites) of the genes that were upregulated in PKO hearts revealed that the top enriched transcription factor binding motifs were the ATF4 and its cofactors C/EBP (CCAAT/enhancer-binding protein) or C/EBP homologous protein binding motifs. DEGs: differentially expressed genes. **D.** qRT-PCR validated the upregulation of classic ATF4 target genes in PKO (red) versus control (Ctrl, blue) hearts at E11.5. n=3–4 per group. **E.** Western blot analysis of ATF4, phosphorylated eIF2α at Serine 51 (Ser51), phosphorylated mTOR at Serine 2448 (Ser2448), and HIF1α, in PKO and Ctrl hearts at E11.5. n=4 per group. **F.** Model for eIF2α -mediated translational control of ATF4 in response to diverse cellular stress responses. **G.** Western blot analysis of ATF4 and phosphorylated eIF2α at Ser51 and ATF4 in *eIF2α*^{S51A} mutant (*Ptpmt1*$^{f/f}$; *eIF2α*$^{m/m}$; *Xml*-Cre^{-}) (S51A), PKO (*Ptpmt1*$^{f/f}$; *eIF2α*$^{+/+}$; *Xml*-Cre^{+}), PKO/*eIF2α*^{S51A} double mutant (dMut) (*Ptpmt1*$^{f/f}$; *eIF2α*$^{m/m}$; *Xml*-Cre^{+}), and control (Ctrl) (*Ptpmt1*$^{f/f}$; *eIF2α*$^{+/+}$; *Xml*-Cre^{-}) hearts at E11.5. n=4 per group. **H.** qRT-PCR analysis of ATF4 target genes in S51A, PKO, dMut, and Ctrl hearts at E11.5. n=3–4 per group. **I.** Heatmap representation of transcript levels of selected ATF4 target genes in S51A, PKO, dMut, and Ctrl hearts at E11.5. **J.** Heatmap representation of transcript levels of selected ER stress-induced genes, including the target genes of ATF4, and XBP1 and ATF6 in PKO and Ctrl hearts at E11.5. **K.** Heatmap representation of transcript levels of selected ATF4 target genes in PKO/GCN2 double knockout (dKO) (*Ptpmt1* $^{f/f}$-*Eif2ak4*$^{-/-}$; *Xml*-Cre^{+}) and wildtype control (WT) (*Ptpmt1* $^{+/+}$-*Eif2ak4*$^{+/+}$; *Xml*-Cre^{-}) hearts (left), and HRI null (HKO) (*Ptpmt1*$^{f/f}$; *Eif2ak4*$^{-/-}$; *Xml*-Cre^{-}), PKO (*Ptpmt1*$^{f/f}$; *Eif2ak4*$^{+/+}$; *Xml*-Cre^{+}), PKO/HRI dKO (*Ptpmt1*$^{f/f}$; *Eif2ak4*$^{-/-}$; *Xml*-Cre^{+}), and Ctrl (*Ptpmt1*$^{f/f}$; *Eif2ak4*$^{+/+}$; *Xml*-Cre^{-}) hearts (right). Note: the genes that encode GCN2 and PTPMT1 are at the same allele, so we could not obtain single knockout littermates. **L.** qRT-PCR analysis of ATF4 target genes in PKO/GCN2 dKO and WT hearts at E11.5, n=5–7 per group. **M.** Western blot analysis of ATF4 and phosphorylated eIF2a at Ser51 in PKO/GCN2 dKO and WT hearts. n=4 per group. **N.** qRT-PCR analysis of ATF4 target genes in HKO, PKO, PKO/HRI dKO, and Ctrl hearts at E11.5, n=3–4 per group. **O.** Western blot analysis of ATF4 and phosphorylated eIF2a at Serine 51 (Ser51) in HKO, PKO, PKO/HRI dKO, and Ctrl hearts. n=4 per group. **P.** Whole embryonic (top) and heart (bottom) morphology of S51A, PKO, dMut, and Ctrl hearts at E13.5. Scale bar: 1 mm. **Q.** Whole embryonic (top) and heart (bottom) morphology of HKO, PKO, PKO/HRI dKO, and Ctrl hearts at E14.5. Scale bar: 1 mm. **R.** qRT-PCR analysis of ATF4 target genes in HKO (*Taz*$^{f/Y}$; *Eif2ak4*$^{-/-}$; *Xml*-Cre^{-}), Tafazzin cardiomyocyte-specific knockout (TKO) (*Taz*$^{f/Y}$; *Eif2ak4*$^{+/+}$; *Xml*-Cre^{+}), TKO/HRI dKO (*Taz*$^{f/Y}$; *Eif2ak4*$^{-/-}$; *Xml*-Cre^{+}), and Ctrl (*Taz*$^{f/Y}$; *Eif2ak4*$^{+/+}$; *Xml*-Cre^{-}) hearts at postnatal day (P) 7. n=3–4 per group. **S.** Western blot analysis of ATF4 and phosphorylated eIF2α at Serine 51 (Ser51) in HKO, TKO, TKO/HRI dKO, and Ctrl hearts at P7. n=4 per group. **T.** Cardiac ventricular weight (VW) to body weight (BW) ratio for HKO, TKO, TKO/HRI dKO, and Ctrl hearts at P7. n= 5–7 per group. **U.** Whole-mount (top) and H&E stained sections (bottom) for HKO, TKO, TKO/HRI dKO, and Ctrl hearts at P8. Scale bar: 1 mm. **V.** Echocardiographic measurements of left ventricular percentage of fractional shortening (% FS) (left), end-diastolic LV internal diameter (LVIDd) (middle), and end-systolic LV

Author Manuscript Author Manuscript Author Manuscript Author Manuscript

internal diameter (LVIDs) (right) for HKO, TKO, TKO/HRI dKO, and Ctrl mice at P7. n = 4–6 mice per group. GAPDH was used as a loading control for western blots. qRT-PCR data were normalized to corresponding 18S levels, and levels in mutants are expressed as the fold-change versus Ctrl. Data are represented as the mean ± SEM. *P < 0.05 PKO, TKO, or dMut, or dKO vs. Ctrl, or as indicated; $^{\#}$P < 0.05 dMut or dKO vs. PKO or TKO, or as indicated, by 2-tailed Student's t test (two group comparison) or two-way ANOVA (four group comparison).